# Manuscript Details

| | |
|---|---|
| **Manuscript number** | IJMS_2016_34 |
| **Title** | Predicted behaviour of QMF systems with and without prefilters using accurate 3D fields |
| **Article type** | Full Length Article |


**Abstract**

Computer simulation enables the effects of a much wider range of design parameters of quadrupole mass filters (QMFs) to be investigated than is economically possible by experiment. Large deviation from ideal behaviour arises from effects of the fringe field regions and is only predicted correctly if the three dimensional fringe fields are determined accurately. The boundary element method, BEM, was used to compute accurate 3D electric fields for complete QMF systems with and without prefilters. Detailed examination of system behaviour without prefilters was used to determine where the effects of fringe fields are particularly detrimental. Examination was extended to systems with prefilters to investigate the required prefilter length and the improvement in performance. The results confirmed that use of a prefilter improves performance in most situations; for high m/z the improvement was large. The results support the original claims of Brubaker although behaviour is more complicated than is described by Brubaker. The results are relevant to QMF designers and users and especially for miniature systems for portable mass spectrometry with the aim to optimise performance whilst maintaining a small instrument footprint.



| | |
|---|---|
| **Keywords** | QMF; Prefilter; Fringe fields; 3-Dimensional |
| **Taxonomy** | Quadrupole Mass Spectrometry, Mass Spectrometry, Modelling, Boundary Element Method |



| | |
|---|---|
| **Corresponding Author** | John Gibson |
| **Corresponding Author's Institution** | University of Liverpool |
| **Order of Authors** | John Gibson, Kenneth Evans, Stephen Taylor |
| **Suggested reviewers** | R. Graham Cooks, Jonathan Batey, Guido Verbeck, Yves ZEREGA |


## Submission Files Included in this PDF

**File Name [File Type]**

Cover.docx [Cover Letter]

JRG_KGE_ST.docx [Manuscript File]

Figure_1.TIF [Figure]

Figure_2.TIF [Figure]

Figure_3.TIF [Figure]

Figure_4.TIF [Figure]

Figure_5.TIF [Figure]

Figure_6.TIF [Figure]

Figure_7.TIF [Figure]

Figure_8.TIF [Figure]

highlights.docx [Highlights]

To view all the submission files, including those not included in the PDF, click on the manuscript title on your EVISE Homepage, then click 'Download zip file'.

Title of paper

# Predicted behaviour of QMF systems with and without prefilters using accurate 3D fields

Authors

John Raymond Gibson,* Kenneth G. Evans and Stephen Taylor

Address for all authors

The Department of Electrical Engineering and Electronics,
The University of Liverpool,
Brownlow Hill,
Liverpool, L69 3GJ, UK

Corresponding author Dr. J. Raymond Gibson
e-mail: jrgjrg@liv.ac.uk

Modelling the behaviour of quadrupole mass filters (QMFs) is undertaken to allow designers to predict the performance of a much wider range of designs than is economically possible by experiment. In the past most models have either ignored or only made approximate estimates of the values and effects of fringe fields. Further there are no accurate electric field computations for QMF systems which incorporate prefilters; these are used in almost all high performance QMF systems. Using the Boundary Element Method (BEM) we are able to include accurate representations of fringe fields and hence accurately predict QMF performance, this has been extended to include QMF systems that include prefilters.

The paper includes detail predictions of the behaviour of QMF systems without prefilters in order to show the adverse effects of fringe fields in detail. The improvement by addition of a prefilter can then be quantified. Knowledge of the detailed effects of fringe fields without a prefilter assists in understanding how a prefilter reduces the adverse effects of fringe fields.

Figures have been included in the main document for refereeing purposes and are also submitted separately in required format.

**Funding.**
This research did not receive any specific grant from funding agencies in the public, commercial and not-for-profit sectors.

# Predicted behaviour of QMF systems with and without prefilters using accurate 3D fields

John Raymond Gibson,* Kenneth G. Evans and Stephen Taylor

The Department of Electrical Engineering and Electronics,
The University of Liverpool,
Brownlow Hill,
Liverpool, L69 3GJ, UK

## ABSTRACT

Computer simulation enables the effects of a much wider range of design parameters of quadrupole mass filters (QMFs) to be investigated than is economically possible by experiment. Large deviation from ideal behaviour arises from effects of the fringe field regions and is only predicted correctly if the three dimensional fringe fields are determined accurately.

The boundary element method, BEM, was used to compute accurate 3D electric fields for complete QMF systems with and without prefilters. Detailed examination of system behaviour without prefilters was used to determine where the effects of fringe fields are particularly detrimental. Examination was extended to systems with prefilters to investigate the required prefilter length and the improvement in performance. The results confirmed that use of a prefilter improves performance in most situations; for high m/z the improvement was large. The results support the original claims of Brubaker although behaviour is more complicated than is described by Brubaker.

The results are relevant to QMF designers and users and especially for miniature systems for portable mass spectrometry with the aim to optimise performance whilst maintaining a small instrument footprint.

Keywords:- QMF, Prefilter, Fringe fields, 3-Dimensional

*Correspondence to:
J. Raymond Gibson,
The Department of Electrical Engineering and Electronics,
The University of Liverpool,
Brownlow Hill,
Liverpool, L69 3GJ, UK
e-mail: jrgjrg@liv.ac.uk

## 1. Introduction

The construction and operation of a quadrupole mass filter, QMF, is well documented in standard references, for example Dawson [1] [2] and Douglas [3]. Computer models are used to predict behaviour of proposed designs allowing design parameters to be investigated more rapidly and at lower cost than is possible experimentally. It is particularly useful for miniature devices as requirements of adequate output signal mean that the ion source has to be proportionally larger for these than for conventional systems and this often has a detrimental effect on performance. It is also possible to use computer modelling to predict the effect of inaccuracies in manufacture.

Conventionally QMF descriptions use rectangular Cartesian coordinates with the system axis coincident with the $z$ axis and electrodes placed symmetrically on the $x$ and $y$ axes. Most predictions of behaviour assume that the electric fields are generated by infinitely long electrodes. In this case the fields only have components in the $x$ and $y$ directions and the electric field in the direction of the $z$ axis, $E_z$, is zero at all positions. Field values for a particular $x,y$ position are the same at all $z$ positions. We refer to such fields as 2D fields.

In practice fields are not ideal because the electrodes have finite length and there are end caps to support the ion source and detector. Most end caps are flat plates with central holes coaxial with the system axis located a short distance from the ends of the quadrupole electrodes. The field extending from the end caps for a distance into the region between the quadrupole electrodes is not ideal. This is the fringe field region in which all components of the field vary in all directions; consequently the axial direction field, $E_z$, is not zero in the fringe field region. We refer to electric fields with components varying in all three coordinate directions as 3D fields.

Predictions using 2D fields provide many indications of QMF design requirements and behaviour; for example minimum electrode length and optimum radius for circular section electrodes. There are large inaccuracies in such treatment; early considerations of deviations from ideal 2D fields are discussed by Dawson [1]. Brubaker [4] [5] [6] suggested that the non-ideal fringe field region at the source end cap led to loss of slow moving ions (heavy ions when operating at constant ion energy). Brubaker introduced the delayed d.c. ramp, implemented using a prefilter, to reduce such effects. Unfortunately much of Brubaker's work is in NASA reports and is not readily available.

We previously described the use of the Boundary Element Method (BEM), formulated as described by Read [7] [8], to determine accurate 3D field values for QMF systems with finite electrode length and end caps [9]. The method avoids the need to differentiate potential distributions produced by other techniques and the inaccuracies this introduces. Using the BEM method fields, except very close to the electrodes, are very accurate.

We have extended the BEM to investigate systems with prefilters. Existing studies of the effects of fringe fields on QMF performance are limited and many ignore the important feature that $E_z$, is not zero. To explain effects observed when a prefilter is included we first examined the effect of fringe fields on behaviour of systems without a prefilter.

## 2. Effects of finite length electrodes and end caps.

The fringe fields at the source end have a very large effect on filter behaviour whereas those at the exit end usually have a small effect which is further reduced if the detector is operated at high voltage. Fringe field effects vary with both geometrical and electrical parameters. It is difficult to give general rules as parameters interact affecting both the transmission of ions through the filter and the peak shape. Our formulation allows the fields to penetrate into the end cap apertures but at present we do not consider ion motion inside the apertures.

There have been several efforts to estimate the effects of finite electrode length and end caps. These involved approximations, for example [2] [6] [10 - 14]. We only know of one set of measurements of the effect of fringe fields on QMF behaviour [15].

Early computations of fringe field effects [6] [10] used a simple linear approximation for the fringe field; all field components were zero at the ion source end cap and changed linearly in the axial direction to the 2D field values over some distance, typically $r_0$. Later work [10] [11] included estimates of the effect of variation in $z$ velocity on individual ion trajectories although the main calculations used constant $z$ velocity. This was stated to be valid provided the ion source has a small radius (small is not defined). Examination of individual ion trajectories shows effects that may be as extreme as ions returning to the source end cap or even oscillating in the z direction; such effects correspond to large changes in the $z$ velocity. It is also noted that there is a discontinuity where the linearly varying field changes to the 2D field; this corresponds to Laplace's Equation not being satisfied.

A more elaborate method [12] [13] used a Liebmann iterative relaxation method to find the potential distribution in the source fringe region of a QMF. The calculations were performed for several values of end gap and the results fitted to an analytical expression. The potential distribution avoids the discontinuity in $E_z$ of earlier work; a weakness is that the distribution does not satisfy Laplace's equation. The effect of the fringe field on motion in the $z$ direction was ignored; the authors state this is adequate for ion source exit radius below $0.1r_0$ whereas we found that this is not generally true as the limit depends on ion velocity (mass for fixed energy), gap size and rf frequency.

Other than our earlier work [9] there appears to be only one other study of QMF behaviour with accurately determined 3D fields [16]; it only gives a limited range of results for one specific system with a prefilter.

Using accurate 3D fields we made extensive studies of QMF behaviour. Example results shown are for a simple system with $r_0$ = 2.6mm, gap from planar end cap surfaces to quadrupole electrodes $0.4r_0$, electrode length $40r_0$. The frequency was 2MHz, the source radius $0.2r_0$ was uniformly illuminated, the detector radius was $r_0$ and the ion injection energy 1eV. Identical results are obtained if the system is scaled as described in Appendix 1 and similar general trends are observed for different parameter values. Figure 1 shows the variation with ion mass of transmission of ions for both 2D and 3D fields using these parameters. Results are shown for hyperbolic cross section electrodes (referred to as hyperbolic) and circular cross section electrodes (circular) with radius $r$=$1.127r_0$ with resolution setting $\eta$ = 0.9992 where $\eta$ = 1.0 corresponds to the scan line passing through the peak of the stability diagram.

All ions start at the exit of the source aperture, have the same energy and initial direction parallel to the filter axis. Initial ion conditions (using uniform distributions of position in source and rf phase) are selected randomly from the infinite set of all possible conditions. Ions are considered to be detected if they reach the central aperture of the detector end cap. Small fluctuations in results may be ignored; they arise because a large, but finite, number of ions are used at each m/z point simulated, typically 50000 to 100000.

The 2D results have the expected form; transmission falls as ion mass increases (ion velocity falls) until it reaches some constant value for hyperbolic electrodes. This is because low mass ions have high velocity and some that have unstable trajectories do not experience a sufficient number of cycles of the rf field to be ejected. However once ions are travelling slowly enough to experience a sufficient number of rf cycles (between 50 and 100 cycles depending on the filter resolution and geometry chosen) and are still within the filter they are in stable trajectories and remain within the filter regardless of how many further cycles they experience. For circular electrodes the transmission is not quite constant as mass increases but ions must experience a very large number of rf cycles for any significant fall in transmission to be observed.

It is very difficult to make direct experimental comparison of the performance with different electrode shapes. The only previous experimental investigations by Brubaker reproduced in [1] (pp129-130) and 2D computations [17] also show that transmission for a system with hyperbolic electrodes is higher than that of a system using circular electrodes.

Results obtained using 3D fields showed very large variations as parameters were changed and were more complicated than for 2D fields. There were also large differences between hyperbolic and circular electrodes using 3D fields. Transmission was usually higher for hyperbolic electrodes but there were situations where the reverse was true. A feature, Figure 1[1], is the variation in the transmission when used in the usual mass spectrometer mode in which ions of all masses have the same energy. The choice of geometric and electrical parameters produces a more pronounced peak than our previous results [9]. The peak position and shape vary with choice of parameters; in particular reduction of the source radius reduces the sharpness of the peak and the peak position moves to a lower m/z value[2]. Variation of transmission in this manner has been previously suggested [1] [11] and is supported by experiment [15]. Dawson [11] only shows a single smooth curve and states that this curve is only an estimate; Ehlert [15] incorrectly thought that the fall in transmission as m/z decreases towards zero was a fault of his instrumentation.

With both hyperbolic and circular electrodes the predicted transmission at low m/z is usually higher for 3D fields than for 2D fields and the 3D transmission increases with m/z in a non-linear manner to a peak value. For m/z above the peak value transmission falls rapidly and behaviour differs markedly for hyperbolic and circular electrodes. At high m/z the transmission using 3D fields is complicated and there are very large variations in both shape and magnitude when any parameter is changed.

Figure 2 shows results using hyperbolic electrodes when some parameters are changed (similar trends are observed for circular electrodes). One trace is the 3D hyperbolic result from Figure 1, the second and third are for ion injection energies of 0.5eV and 4eV instead of 1eV. The fourth trace is for a frequency 1MHz instead of 2MHz with ion energy 1eV. The fifth and sixth have the source to end gap doubled to $0.8r_0$ (long gap) and are for 2MHz and 1MHz respectively with ion energy 1eV. These results confirm the analysis in Appendix 1. For 2MHz operation with 0.5ev, 1eV and 4eV ion energy (and any other ion energy) using a gap of $0.4r_0$ the peak occurs at an ion velocity of approximately $2640 ms^{-1}$, that is 0.081 in normalised units of $r_0 x rad^{-1}$, and the traces are identical except for movement on the logarithmic m/z axis Also the 2MHz results at 0.5ev and 4eV are identical as for these $C_E = C_\omega$ ($C_E$ and $C_\omega$ are defined in Appendix 1); the 4eV values are shown with a small offset to accommodate this.

There are large variations in the transmission curves if parameters; especially source gap, source radius and ion energy; are changed although the overall behaviour is similar.

## 3. The fringe field

Any definition of the fringe field length is arbitrary. The fringe field length is infinite but there will be a distance into the region between the filter electrodes at which its effect becomes negligible. As the difference between predictions using 2D and 3D fields arises from the fringe fields we examined the distance over which the fringe field has a significant effect.

We ignore ion motion in the fringe fields inside the end cap apertures by starting ions at the exit of the source end cap and detecting them at the entrance to the detector end cap. Two methods were used to estimate the distance over which the fringe field results for transmission differ significantly from results using 2D fields. One method determined the gradient of $E_x$ or $E_y$ at many axial positions within a radial distance $0.5r_0$ from the $z$ axis; the gradient should be 2.0 at all positions for infinite length hyperbolic electrodes with unit applied potential and unit field radius. The results indicated that variation of the field components was too small to affect ion transmission by a measurable amount for most of the filter length; significant variations are only found near the end caps. Choosing a decrease of 0.1% in the gradient as the fringe field limit showed that the fringe field length (source exit plane, through the gap, and into region inside filter electrodes) varies from approximately $1.5r_0$ to $2r_0$ for end gaps up to about $1.0r_0$.

[1] All the results presented for transmission and loss are values at the maximum of the mass peak.
[2] m/z in units Da is commonly used to indicate the position on the $x$ axis of a mass spectrometer scan. Note that the z in this term is not the Cartesian coordinate giving the distance along the system axis which is also denoted as z.

The second method used the change of peak transmission for a very long filter when, instead of starting at the source exit, the ions start in a plane moved in the positive $z$ direction. When the starting plane was more than $2.5r_0$ from the source end cap the transmission is found to be identical to that observed using 2D fields. As the starting plane was moved closer to the source the predicted transmission increased. Again a choice of the value of increase was used to define the fringe field boundary. A value of 0.35% gave results matching the first method when that used a field variation of 0.1%. Results for a transmission increase of 0.6% are close to those in Table 1 of McIntosh and Hunter [13]. Investigations indicated that the fringe field length is somewhat larger than the value of $r_0$ implied by Dawson [11] and varies with gap, source radius and resolution setting.

Brubaker's patent [4] claims that the loss of heavy (low velocity) ions is due to ion motion in the $y$ direction in the fringe field region being outside the region of stability. This is not strictly correct as the concept of a simple stability diagram that describes operation in the region of 2D fields does not apply in the fringe field region. The equations of motion indicate that ions are accelerated more strongly away from the axis in the $y$ direction than in the $x$ direction in the fringe field region; this strong acceleration in the $y$ direction leads to significant loss of low velocity ions.

Figure 3 shows the percentage of ions lost in each coordinate direction, including the $z$ direction, as well as the percentage transmitted for the hyperbolic QMF without a prefilter. An important feature is that a large proportion of low velocity ions are lost by returning to the source end cap; clearly any model that ignores changes in $z$ velocity will not predict this effect. This loss by reversing direction decreases as the ion source diameter is reduced but is not zero for any finite diameter.

As the axial direction injection velocity increases (m/z decreases) the proportion of ions that return to the end cap drops while the proportion lost in the $y$ direction increases. Eventually the proportion lost in the $x$ direction begins to rise and later again the proportion lost in the $y$ direction falls. At high velocities no ions return to the end cap and the proportions lost in $x$ and $y$ directions are similar. Changing parameters such as end gap, frequency, source radius and resolution changes the detailed form of the results but the general trends remain the same. On the low mass side of the peak losses in the $y$ direction are higher than at the peak and losses in the $x$ direction are higher on the high mass side.

We have investigated a large range of parameters. It was not possible to determine simple rules describing QMF behaviour when modelled using accurate 3D fields but the following points describe common behaviour. Ion velocity is used here as the independent variable rather than ion mass as behaviour depends principally on the time taken to pass through the fringe field region. In normal mass scan operation lower velocity corresponds to higher mass.

- The inclusion of fringe fields in predicting QMF behaviour usually leads to higher transmission for high velocity ions but lower transmission for low velocity ions compared with predictions ignoring fringe fields.
- There is a peak in transmission as a function of ion velocity. For a particular length gap between end cap and filter electrodes peak position usually corresponds to ions being in the fringe field for a time between 0.6 and 1.5 periods of the rf.
- The transmission also depends on the ion source characteristics for an actual QMF and on the model of the ion source used in any computer simulation that includes fringe fields. The radius of the ion source has a strong effect on the transmission characteristic.
- Mass peak shape varies with ion velocity to a greater extent when the effects of fringe fields are included than when they are ignored. The variation in peak shape may cause a variation in resolution as a function of ion velocity.
- Brubaker's claim that low transmission of low velocity ions is caused by acceleration in the $y$ direction in the fringe field is confirmed. This acceleration either leads directly to loss in the $y$ direction or causes ions to move to a position of stronger axial rf field which causes some to return to the source end cap.

- Fringe field length cannot be described by a single value. Fringe fields have no significant effect on ion motion after a distance of between $1.5r_0$ and $2.5r_0$ into the region between the electrodes; the exact distance depends on all parameters.

## 4. Behaviour of QMF systems with a prefilter

The fringe field between the source end cap and the quadrupole electrodes has the adverse effect of producing a large drop in transmission for low velocity ions. Brubaker [4] [5] increased the transmission by addition of a delayed d.c. ramp using a prefilter; one is now used in most high performance QMF systems.

Brubaker [4] [5] [6] used at least two prefilter designs that are shorter than most used in modern systems; he also introduced an alternative form [18]. Most modern prefilters consist of four additional electrodes with the same cross section as the main filter electrodes and aligned with them. The prefilter electrodes are placed between the source end cap and the main electrodes and are operated with only the rf voltages applied to the electrodes (no d.c.) or with the rf voltages and the same small d.c. voltage applied to all electrodes rather than opposite polarity d.c. voltages on *x* and *y* electrodes.

The program to determine QMF behaviour using 3D fields was modified to include a prefilter. Electric fields are linear in the sense that they satisfy the requirements of superposition; fields can be determined for several different conditions and superimposed. As in [9] we used the BEM with each electrode (including the prefilter electrodes and end caps) modelled by sets of charges determined by solving Laplace's Equation with boundary conditions set by the potentials at the electrode surfaces. Solutions were performed three times. Once with voltages of +1 on the main filter *x* electrodes and -1 on the *y* electrodes and with zero on all other electrodes including the end caps. The second solution had +1 on the prefilter *x* electrodes and zero elsewhere, and the third had -1 on the prefilter *y* electrodes and zero elsewhere. The separate solutions for the prefilter *x* and *y* electrodes allow a common d.c. bias to be applied to prefilter electrodes. Ions were traced through the system as previously except that at each point the fields were the sum of those produced by all three solutions with each multiplied by the appropriate electrode voltage. It is straightforward to modify this to include a bias on end caps or displaced electrodes by additional solutions of Laplace's Equation.

Compared with a simple QMF additional parameters affect the behaviour of a system with a prefilter. These are the prefilter length, the gap between the source end cap and the prefilter, and the gap between the prefilter and the main electrodes. Some systems also apply a small common constant voltage to all prefilter electrodes; our simulations allow inclusion of this bias but it has not been investigated at present.

There are only a few published studies of the manner in which a prefilter affects QMF behaviour; other than the original publications by Brubaker [4] [5] [6] we are only aware of brief comments by Arnold [19], a short sequence of papers by a Hungarian group [20] – [24], a later paper by Takebe et.al [25], and the work of Wright et.al [26]. Hiroki et.al. [27] investigated operation in the upper stability zone which is not examined here.

To study the action of a prefilter but restrict the very large number of cases we first investigated the effect of varying the prefilter electrode length by adding a prefilter to the hyperbolic QMF used to produce Figure 1. The three gaps in the axial direction were all $0.4r_0$. Transmission from source to detector was examined for a range of prefilter lengths. Figure 4 shows a selection of the results and includes the previous results without a prefilter for comparison; a logarithmic scale is used for the m/z axis to show a wide range of values. All results are for 1eV ions, frequency 2MHz and $\eta = 0.9992$.

The analysis in Appendix 1 stating that identical behaviour is obtained if the parameter $\lambda$ (equation 5) is constant applies to a system with a prefilter provided the rf frequency on the prefilter is the same as that on the main electrodes. Transmission results change if the value of $\lambda$ changes or if the ion source exit radius or any of the gaps change. The results suggest that a prefilter length of $4r_0$ is probably adequate for the system modelled. If system construction allows, a longer prefilter than the minimum slightly improves performance

and reduces the value of m/z at which oscillatory behaviour becomes significant. For the following results a prefilter length of $6r_0$ was used with the same parameters as previously except as indicated.

When a prefilter was added to a QMF the maximum transmission predicted as m/z varied was higher and the maximum occurred at a higher m/z value than without a prefilter.

Without a prefilter the size of the gap between the source end cap and the main filter electrodes had a large effect on system behaviour. With a prefilter the size of the gap between the source end cap and prefilter electrodes had little effect unless the gap was large, typically over $r_0$, or the ion beam was strongly divergent. For divergent ion beams loss increased as the gap increased as is expected.

Systems with a prefilter also have a gap between the prefilter and the main QMF electrodes. The effect of varying this gap was examined for a prefilter of length $6r_0$ with m/z values above the region where there are large fluctuations in transmission. Transmission was not affected by the gap between prefilter and main filter until the gap was increased to about $1.2r_0$ which is larger than is commonly used. When the gap exceeded about $1.4r_0$ transmission was greatly reduced.

When ions have high velocity, low m/z, the fluctuations in transmission as m/z is varied reduce the usefulness of the system; effects on resolution are variable although resolution is at least that without a prefilter. Generally systems with prefilters are used for investigations at relatively high m/z values so the region with fluctuations in transmission was not investigated in detail. Above the region with fluctuating transmission, the prefilter improves resolution. Although the width at the peak base is little changed by the prefilter the peak height is greater; using any of the common definitions of resolution the resolution is improved. More importantly, if operation is limited by detector sensitivity then the higher transmission with a prefilter allows operation at higher resolution setting and hence much greater resolution can be achieved. It was found that there was often an improvement in the peak shape with a prefilter. Two examples comparing peak forms with and without a prefilter are shown in Figure 5 (peak transmission is at about $1000ms^{-1}$ for the system modelled) and include results without a prefilter scaled for comparison.

**5. Discussion of predictions**

Brubaker's claim that slow moving ions are lost because there is increased acceleration (Brubaker often uses the term impulse) in the $+y$ and $-y$ directions in the fringe field is supported by the simulation results. Figure 6 illustrates simulation results for transmission and loss for the previously defined systems; the prefilter results are shown for two diameters of ion source.

Ions are defined as lost in the $x$ direction if the distance of the ion from the axis exceeds $r_0$ in either the positive or negative $x$ direction; similarly loss in the $y$ direction corresponds to $|y|$ exceeding $r_0$. Loss by reflection, that is loss in the $z$ direction, is when ions return to the source end cap position.

The simulation program indicated the direction of loss for each ion and the distance travelled before it was lost. For loss in $x$ or $y$ directions the distance is from the source end cap to the $z$ position at which the $x$ or $y$ distance from the axis exceeds $r_0$. For loss by reflection it is the furthest distance the ion travels in the $z$ direction. Figure 7 shows the position in the axial direction at which ions were lost in units of $r_0$ for two values of m/z with and without a prefilter. Results are only shown from the source to the point in the main filter after which there is very little further ion loss. For the resolution used more than 99.9% of the total ion loss at the mass peak occurs in a distance less than $10r_0$ into the main filter; the further small loss occurs close to the exit end of the main filter. The number of ions lost at each $z$ position was determined by dividing the axial direction into intervals of $0.002r_0$ and the fraction of the total number of ions in every interval was determined for each loss mechanism. Figures 6 and 7 are for one QMF design with and without a prefilter; similar trends were observed for other designs and operating conditions.

For the example without a prefilter loss in the $y$ direction increases rapidly as m/z increases up to m/z ≈ 80Da; above 80Da loss in the $y$ direction falls and loss by reflection increases with the total of the two about 90%

of all ions. Losses in the *x* direction are slightly larger than those in the *y* direction at very low m/z but fall rapidly as m/z increases.

Without a prefilter ions were lost in the *x* or *y* directions at a distance of between about $r_0$ and $5r_0$ into the filter. Ions lost by reflection travelled a distance less than $1.5r_0$ into the filter at low values of m/z; as m/z was increased loss by reflection increased, the peak moved closer to the source and a second small peak occurred very close to the source in the fringe field.

Transmission with a prefilter was higher than without except for a few very low m/z values in the region where transmission fluctuates rapidly. Above m/z ≈ 80Da (the position of maximum transmission without a prefilter) transmission was always larger with a prefilter; about a factor of ten for the example. Up to the m/z value at which loss by reflection became significant most ion loss occurred in the main filter near the entrance end. Although the losses were much smaller than without a prefilter the relative proportions lost in each direction and the positions at which ions were lost were similar. When loss by reflection became significant, at around m/z = 100Da for the example, further increase in m/z led to reduction in losses in the *x* and *y* directions and increased loss by reflection. The increasing loss by reflection occurred at both the entrance to the main filter and the entrance to the prefilter; at high m/z values loss at the prefilter entrance became the main loss mechanism.

Ion motion in the fringe fields is very complicated and the results show that change in velocity in the *z* direction cannot be ignored. Also the fringe fields in the transverse directions cannot be regarded as scaled versions of the ideal quadrupole field.

As Brubaker [4] [5] suggested, the d.c. component of the bias on the main filter electrodes has a large effect in the fringe field region. This d.c. field combines with effects of the rf field in a complicated manner. The potentials applied to the rods are designed to control the *x* and *y* components of field in the filter but have the side effect of producing an axial field distribution in the fringe region. If ions pass quickly through the fringe field the rf potential applied to the rods can accelerate or decelerate the ions axially depending upon the starting position and the phase of the rf at the time of injection.

The approximate pseudopotential well model used to predict ion trap performance [28] [29] shows that ions in a one dimensional rf field of varying strength move towards the area of lowest field strength. This corresponds to one of the mechanisms for reflection of ions in the fringe field of a quadrupole system. However, the mechanisms that cause ions to return to the source are generally more complicated than this. Detailed inspection of trajectories shows that the motion in the three coordinate directions is strongly coupled throughout most of the fringe region; this can result in rf oscillations in the *x* and *y* directions generating a net force in the z-direction, toward the source, when averaged over each rf cycle. The expansion of the ion beam in the y direction in the fringe field is particularly effective in accelerating ions back toward the source. The fringe fields in all three component directions are weaker close to the axis hence reducing the source radius reduces the strength of the field the ions experience in the fringe region. The trajectories are less disturbed during transit through the fringe field; with a prefilter behaviour becomes closer to direct injection from the source into the 2D region of the prefilter. After passing through the prefilter ions reach the second fringe region with a reduced radius resulting in reduced losses and increased transmission. Note that the example results use the same total ion current which means the ion density in the source is higher when the source is smaller (more ions are close to the axis).

A conspicuous feature of the results is the fluctuation in transmission with variation in m/z at low values when there is a prefilter; this has been observed previously [23]. Alternatively, variation in ion velocity by changing ion energy produces the same fluctuations [24]. Many measurements of features of rf-only quadrupoles show some form of fluctuating behaviour, for example [22] [25] [26] [30 - 33]. Simulations of 2D hyperbolic rf-only quadrupoles show that the ion beam amplitude expands and contracts as ions travel through the system. Appendix 2 describes this behaviour and explains why it occurs. It also describes why the fringe fields both between source end cap and prefilter and between prefilter and main filter modify this and lead to the fluctuations decreasing as m/z increases. The intervals between the peaks for prefilter length $6r_0$ (and to a slightly poorer degree for length $12r_0$ in Figure 4 correspond to the periodicity of the maxima

and minima in the rf-only prefilter of $\Omega = (1 - \beta)\,\omega_f$ determined in Appendix 2. Agreement is poorer for shorter prefilters as the fringe fields are a large proportion of the total prefilter length.

## 6. Conclusions

Using accurate 3D fields the performance of QMF systems with and without prefilters has been examined. There are only limited measurements available that vary parameters in the manner possible with a computer model but, for the few available measurements, the computer predictions using accurate 3D fields are able to reproduce all the observed effects.

While predicted behaviour varied with many parameters it was clear that Brubaker's original objective of increased transmission for low velocity (high m/z) ions was achieved by adding a prefilter to a QMF. The transmission increase was usually large, at least an order of magnitude. In addition to Brubaker's claim that the prefilter reduces loss of ions because of an 'impulse' in the *y* direction in the fringe field there is also a significant reduction in the number of ions reflected back to the source in the fringe field region. There is a small improvement in resolution, higher resolution operation is possible, and there is often an improvement in peak shape.

Using the simulation program it is possible to suggest a minimum prefilter length provided electrode size, rf frequency and ion energy have been chosen.

For low m/z, high velocity, ions the behaviour of systems with prefilters is complicated exhibiting '*fluctuations*' in transmission as a function of ion velocity. Such fluctuations are related to properties of rf-only quadrupoles described in Appendix 2. The effects are of interest in understanding prefilter behaviour but are of less concern in practice as most prefilters are used to improve the QMF performance for heavy, low velocity, ions. Observed fluctuations will be smaller than predicted because the ions will have a spread in energy and initial direction; they could be reduced by deliberately modulating the ion energy to smooth the response. Alternatively, as suggested in [24], the ion energy could be adjusted so that transmission was always at a maximum position.

The largest effect that is not included in the present simulations is that caused by variation in ion source characteristics. The results described here use a uniformly distributed beam of ions parallel to the system axis with all ions having identical energy; this allows effects of varying system parameters to be determined. Most QMF systems include some form of focussing of the ion beam, there are often space charge effects in the exit region of the ion source and the ions have a small spread of energies. Although not described here we obtained similar trends in behaviour with simple alternative forms of ion beam and some indication that the prefilter reduces the dependence of system behaviour on the ion beam form. Ideally a complete model of a QMF system should include an accurate model of the ion source including space charge effects. This modelling is difficult and the only attempts at ion source modelling for QMF systems appear to be those of Allison's group [34] [35] and Langridge [16].

## Appendix 1

The equation of motion of an ion under the influence of a time varying electric field is

$$m\frac{\mathrm{d}^2\mathbf{r}}{\mathrm{d}t^2} = Q\mathbf{E} \qquad (1)$$

where $m$ is the ion mass and $Q$ its charge. The electric field, **E,** is a functions of the spatial components, **r**, and time, $t$. For a QMF, even if imperfect, the electric field is

$$\mathbf{E} = V\mathbf{E}_0(\mathbf{r})\left(\frac{U}{V} - \cos\left(\omega_f t + \phi\right)\right) \qquad (2)$$

$U$ is the d.c. voltage and $V$ is the amplitude of the rf voltage with angular frequency $\omega_f$ applied to the electrodes. $\mathbf{E}_0$ (**r**) is the field at any position **r** when $V = 0$ and $U = 1$.

Normalise spatial dimensions using $\boldsymbol{\xi} = \mathbf{r}/r_0$ and time[3] using $\boldsymbol{\tau} = \omega_f t$ then the normalised field $\boldsymbol{\varepsilon}(\boldsymbol{\xi},\boldsymbol{\tau})$ in units of volts/$r_0$ is

$$\boldsymbol{\varepsilon}\left(\boldsymbol{\xi},\tau\right) = r_0\mathbf{E}_0(\mathbf{r})\left(\frac{U}{V} - \cos\left(\omega_f\tau + \phi\right)\right) \tag{3}$$

From (1), (2) and (3) the equation of motion in normalised units may be written

$$\frac{\mathrm{d}^2\boldsymbol{\xi}}{\mathrm{d}\tau^2} = \lambda\varepsilon(\boldsymbol{\xi},t) \tag{4}$$

where $\lambda$ is the dimensionless constant

$$\lambda = \frac{QV}{m\omega_f^2 r_0^2} \tag{5}$$

Note that the normalised velocity, $\frac{\mathrm{d}\boldsymbol{\xi}}{\mathrm{d}\tau}$, is related to the actual velocity, $\frac{\mathrm{d}\mathbf{r}}{\mathrm{dt}}$, by

$$\frac{\mathrm{d}\boldsymbol{\xi}}{\mathrm{d}\tau} = \frac{1}{\omega_f r_0}\frac{\mathrm{d}\mathbf{r}}{\mathrm{d}t} \tag{6}$$

If equation (4) is solved to determine ion trajectories for various combinations of the parameters identical solutions will be obtained for all ions for which the value of $\lambda$ is the same provided the initial conditions are the same. Identical initial conditions require that the initial normalised values of position $\mathbf{r}$, ion velocity $\frac{\mathrm{d}\boldsymbol{\xi}}{\mathrm{d}\tau}$, and phase $\varphi$ must be the same.

Two ions, indicated by subscripts 1 and 2, will follow identical normalised trajectories provided λ is the same, this requires that

$$\frac{V_1}{m_1\omega_1^2} = \frac{V_2}{m_2\omega_2^2} \tag{7}$$

For the normalised initial velocities to be identical requires

$$\left(\left.\frac{\mathrm{d}\boldsymbol{\xi}}{\mathrm{d}\tau}\right|_{\tau=0}\right)_1 = \left(\left.\frac{\mathrm{d}\boldsymbol{\xi}}{\mathrm{d}\tau}\right|_{\tau=0}\right)_2 \tag{8}$$

Hence from (6) and (8)

$$\frac{1}{\omega_{f1}}\left(\left.\frac{\mathrm{d}\mathbf{r}}{\mathrm{d}t}\right|_{t=0}\right)_1 = \frac{1}{\omega_{f2}}\left(\left.\frac{\mathrm{d}\mathbf{r}}{\mathrm{d}t}\right|_{\tau=0}\right)_2 \tag{9}$$

If the injection energies differ by a factor $C_E$ then

$$C_E\frac{m_1}{2}\left(\left.\frac{\mathrm{d}\mathbf{r}}{\mathrm{d}t}\right|_{t=0}\right)_1^2 = \frac{m_2}{2}\left(\left.\frac{\mathrm{d}\mathbf{r}}{\mathrm{d}t}\right|_{t=0}\right)_2^2 \tag{10}$$

From (9) and (10)

$$C_E m_1\omega_{f1}^2 = m_2\omega_{f2}^2 \tag{11}$$

For identity (11) to hold (7) requires that $C_E V_1 = V_2$

A simulated QMF mass peak is obtained by finding the trajectories of a large number of ions for a range of values of $V$ ($V$ is varied to perform the scan across the mass peak) and hence, from (5), a range of values of $\lambda$. The ions must have a spread of starting conditions of initial $x$ and $y$ position in source disc, initial velocity which may have components in all three component directions, and rf phase angle at time of leaving the source. Provided that large numbers of ions with randomly selected starting conditions are chosen from the

3. Note that Dawson [1] uses normalisation which differs by a factor of 2

same distributions there will be matching pairs of ions in each of the sets with the same value of $\lambda$. Therefore exactly the same mass peak will be produced for any pair of cases where (11) holds. For example if $\omega_{f2} = 2\omega_{f1}$ and ions of both masses have the same energy then exactly the same transmission characteristic will be produce as for $\omega_{f1}$ provided $m_2 = 0.25m_1$.

If the two characteristics are also obtained for frequencies different by a factor $C_\omega$ such that

$$\omega_{f2} = C_\omega \omega_{f1} \tag{12}$$

then from (11) and (12)

$$\frac{m_2}{m_1} = \frac{C_E}{C_\omega^2} \tag{13}$$

Thus if $C_E = C_\omega$ the transmission characteristics will be identical. If $C_E \neq C_\omega$ and the transmission characteristics are plotted using a logarithmic scale for the m/z axis the characteristics will be identical except for a horizontal shift.

## Appendix 2

The fluctuations in transmission produced when an rf-only prefilter is added to a QMF can be explained by examining the rf-only case of a 2D quadrupole with hyperbolic electrodes. The $x$ and $y$ trajectories of ions are described by the Mathieu equation; the Floquet solution for stable trajectories may be written as a sum of sinusoids.

$$\alpha(t) = A\sum_{n=-\infty}^{\infty} C_{2n}\cos((n+\frac{\beta}{2})\omega_f t + \psi_{2n}) \tag{14}$$

with

$$\psi_{2n} = \left(n+\frac{\beta}{2}\right)\phi + \theta \tag{15}$$

$\alpha$ is either $x$ or $y$, $\omega_f$ is the angular frequency of the applied rf, $\phi$ is the rf phase at the time the ion enters the field, $\beta$ is the characteristic exponent of the Mathieu equation, $A$ and $\theta$ are constants of integration that depend on initial conditions.

The coefficients $C_{2n}$ are functions of $a$ and $q$ only ($a$ and $q$ are defined in the usual manner); for the rf-only case $a = 0$ and the coefficients only depend on $q$. $C_{2n}$ and $\beta$ can be determined by direct calculation (see [1]).

The sinusoids have frequencies $(n + \beta/2)\ \omega_f$. The trajectories are oscillatory but not periodic because the frequencies of the components are not harmonically related. For the first stable region $\beta$ may have any value from zero to one. Therefore the frequencies are not the applied frequency or harmonically related to it except in special cases where $\beta$ is any rational fraction, for example $1/2$. For normal QMF operation with q ≈ 0.706 $\beta$ is about 0.57. The $C_{2n}$ coefficients decrease as $|n|$ increases so, although the trajectories are not periodic, when they are plotted over a short time interval they do appear to be periodic with frequency $0.5\beta\omega_f$.

For our simulations ions start at any $x,y$ position within the source exit aperture. They also have any possible phase angle relative to the applied rf and all positions within the source and all initial phase angle are equally probable. However this does not correspond to all possible phase angles, $\psi_{2n}$, relative to frequencies $(n + \beta/2)\ \omega_f$. Simulations using a large number of ions and 2D fields show that $\psi_0$ lies within two bands, Figure 8a, each approximately two radians wide. One band is for ions with positive initial displacement $\alpha$; the other band for ions with negative initial displacement is displaced by $\pi$ radians. This banding of the phases causes the trajectories of the ions to have their maximum and minimum displacements grouped at regular intervals along the z axis.

The variation of the spread of the trajectories may be characterised by calculating the root mean square, RMS, value of the lateral displacement, $\alpha_{rms}$, at each instant of time for a large number, $M$, ions with randomly selected initial conditions as

$$\alpha_{rms}(t) = \left( \frac{1}{M} \sum_{m=1}^{M} \alpha_m(t)^2 \right)^{\frac{1}{2}} \quad (16)$$

where $\alpha_m(t)$ is the trajectory of the $m^{th}$ ion (equation 14).

Since $\alpha(t)$ has many sinusoidal components $\alpha_{rms}(t)$ will be the sum of a constant plus sinusoids at all harmonic frequencies of all components and also at sum and difference frequencies. The amplitudes of the resulting components of $\alpha_{rms}(t)$ are determined by the amplitudes of the components of $\alpha(t)$ and by the phases of these components. Figure 8b shows example 2D field simulations for $q = 0.706$, m/z = 100Da, energy 1eV, $r_0 = 2.6$mm, source radius $0.2r_0$ and frequency 2MHz. Many simulations with 2D fields were performed and showed that $\alpha_{rms}(t)$ is dominated by the component at frequency $\Omega$ given by $\Omega = (1 - \beta)\,\omega_f$; this is the difference frequency from components of $\alpha(t)$ with $n$=0 and $n$=-1. Note that some authors [26] [28] incorrectly imply that the dominant frequency is $\beta\omega_f$; for the rf-only case when the QMF is operated with $q = 0.706$ then $\beta \approx 0.57$ so the difference is small.

The axial distance between successive minimum (or maximum) values of $\alpha_{rms}$ is

$$D = \frac{2\pi v_z}{\Omega} \quad (17)$$

where $v_z$ is the mean axial velocity and $\Omega = (1 - \beta)\,\omega_f$ is the dominant frequency of $\alpha_{rms}$. For ions with mass $m$ and injection energy $V_i$eV then

$$D = \frac{2\pi}{\Omega} \sqrt{\frac{2QV_i}{m}} \quad (18)$$

The 2D field simulations also indicate that the spread is always at a minimum at the source hence the spread will be minimum at the end of the prefilter whenever the prefilter length is an integral multiple of $D$. When operating with constant ion energy the velocity varies with m/z hence the *'size'* of the beam entering the main filter varies producing the fluctuations in transmission as a function of m/z.

Equation 17 assumes that all ions have the same axial velocity $v_z$. For a 3D field transmission through the source fringe region results in a spread in ion velocities causing the positions of successive minima (or maxima) to become less pronounced as distance from the source increases. The reduction increases as the number of minima in the prefilter increases, that is as m/z increases, and eventually at high enough m/z the variation in ion beam size is very small and the fluctuations are no longer present.

References


[1] P.H. Dawson, Quadrupole Mass Spectrometry and Its Applications, Elsevier, Amsterdam (1976)

[2] P.H. Dawson, Ion optical properties of quadrupole mass filters, Adv. Electron. Electron Phys. 53 (1980) 153–208

[3] D.J. Douglas, Linear quadrupoles in mass spectrometry, Mass Spectrom. Rev. 28 (2009) 937–960

[4] W.M. Brubaker, Auxiliary electrodes for quadrupole mass filters, US Patent 3129327 (1964)

[5] W. M. Brubaker, A study of the introduction of ions into the region of strong fields within a quadrupole mass spectrometer, Quarterly report NASA Contract NASW-1298 (1965)

[6] W. M. Brubaker, An improved quadrupole mass analyser, Adv. Mass. Spectrometry 4 (1968) 293–299

[7] F.H. Read, 'Zero gap' electrostatic aperture lenses, J. Phys. E 4 (1971) 562–566

[8] F.H. Read, A. Adams, J.R. Soto-Montiel, Electrostatic cylinder lenses. I. Two element lenses, J. Phys. E 4 (1971) 625–632

[9] J.R. Gibson, K.G. Evans, S.U. Syed, S. Maher, S. Taylor, A method of computing accurate 3D Fields of a quadrupole mass filter and their use for prediction of filter behaviour, J. Am. Soc. Mass Spectrom. 23 (2012) 1593-1601

[10] Dawson, P.H. Fringing fields in the quadrupole mass filter, International J. Mass Spectrom. Ion Phys. 6, 33-44 (1971)

[11] P.H. Dawson, The acceptance of the quadrupole mass filter, International J. Mass Spectrom. Ion Phys. 17 (1975) 423-445

[12] K.L. Hunter, B.J. McIntosh, An improved model of the fringing fields of a quadrupole mass filter, Int. J. Mass Spectrom. Ion Proc. 87 (1989) 157–164

[13] B.J. McIntosh, K.L. Hunter, Influence of realistic fringing fields on the acceptance of a quadrupole mass filter, Int. J. Mass Spectrom. Ion Proc. 87 (1989) 165–179

[14] A.E. Banner, The effects of entrance fields on the performance of quadrupole mass spectrometers, European Journal of Mass Spectrometry 15 (2009) 445-458

[15] T.C. Ehlert, Determination of transmission characteristics in mass filters, J. Phys. E. 3 (1970) 237-9

[16] D.J. Langridge, 3D Simulation of Quadrupole Mass Filters with Offset and Tilted Rods, 62nd ASMS Conference Baltimore (2014)

[17] J.R. Gibson, S. Taylor, Prediction of quadrupole mass filter performance for hyperbolic and circular cross section electrodes, Rapid Commun. Mass Spectrom. 14 (2000) 1669–1673

[18] W. M. Brubaker, A new approach to the implementation of a delayed DC ramp quadrupole mass filter, J. Appl. Phys. Suppl.2, Pt. 1 (1974) 179-181

[19] W. Arnold, Influence of segmented rods and their alignment on the performance of a quadrupole mass filter, J.Vac.Sci.Tech 7 (1970) 191-194

[20] C. Trajber, M. Simon, M. Csatlos On the use of prefilters in quadrupole mass spectrometers, Meas. Sci. Technol 2 (1991) 785-787

[21] C. Trajber, M. Simon, S. Bohátka, A method for uniform optimisation of quadrupole prefilters, Rapid Commun. Mass Spectrom. 6 (1992) 459-462

[22] C. Trajber, M. Simon, S. Bohátka, I. Futó, Mass independent prefilter arrangement for quadrupole mass spectrometer, Vacuum 44 (1993) 653 -656

[23] M. Simon, S. Bohátka, C. Trajber, I. Futó, Experimental verification of an improved prefilter model. Rapid Commun. Mass Spectrom. 9 (1995) 629-633

[24] M. Simon, I. Futo, The effect of fringing field on the transmission of the prefiltered quadrupole mass spectrometers, Vacuum 50 (1998) 305-311

[25] M. Takebe, S. Kumashiro, Computer simulation of the quadrupole mass filter, Nucl. Instr. Meth. Phys. Rev. A 363 (1995) 411-415

[26] S. Wright, S. O'Prey, R. R. A. Syms, G. Hong, A.S. Holmes, Microfabricated quadrupole mass spectrometer with a Brubaker prefilter. J. Microelectromech. Syst. 19, (2010), 325-337

[27] S. Hiroki, K. Sakata, S. Muramoto, T. Abe, Y. Murakami, Effect of a prefilter on the sensitivity of a high-resolution quadrupole mass spectrometer, Vacuum 40 (1996) 681-683

[28] R.F. Wuerker, H. Shelton, R.V. Langmuir, Electrodynamic containment of charged particles, J.Appl. Phys 30 (1959) 342-349

[29] F.G. Major, H.G. Dehmelt, Exchange-collision technique for the rf spectroscopy of stored ions, Phys. Rev. 170 (1968) 91-107

[30] P. E. Miller, M. Bonner Denton, The transmission properties of an rf-only quadrupole mass filter, Int. J. Mass Spectrom. Ion Proc 72 (1986) 223-238

[31] F. Muntean, D. Ursu, N. Lupsa, Ion trajectory analysis for rf-only quadrupoles, Vacuum 46 (1995) 131-137

[32] F. Muntean Transmission study for rf-only quadrupoles by computer simulation, Int. J. Mass Spectrom. Ion Proc 151 (1995) 197-206

[33] J. Wei, Transmission Characteristics of RF-Only Devices: Quadrupoles and Octupoles as Ion Pipes, 46th ASMS Conference Orlando (1998)

[34] M. C. Cowen, W. Allison, J. H. Batey, Electron space charge effects in ion sources for residual gas analysis, Meas. Sci. Technol. 4 (1993) 72-78

[35] M. C. Cowen, W. Allison, J. H. Batey, Nonlinearities in sensitivity of quadrupole partial pressure analyzers operating at higher gas pressures, J. Vac. Sci. Technol. A 12 (1994) 228 – 234

**Captions for Figures**

Figure 1 Predicted peak transmission as a function of ion mass; (b) is the low m/z region expanded.

Figure 2 Peak transmission with varying energy, frequency and end gap (4eV offset so visible).

Figure 3 Direction in which ions are lost (at mass peak); (b) is the low m/z region expanded.

Figure 4 Peak transmission for several lengths of prefilter.

Figure 5 Mass peak profiles, m/z = 100Da. a) 1eV, $\eta = 0.9992$, velocity 1384 ms-1; b) 0.1eV, $\eta = 0.9999$, velocity 438 ms-1 (amplitude scales differ).

Figure 6 Transmission and loss for systems with and without a prefilter.

Figure 7 Position at which ions are lost. (a) m/z = 60Da, no prefilter. (b) m/z = 280Da, no prefilter. (c) m/z = 60Da, with prefilter. (d) m/z = 280Da, with prefilter. The short vertical lines indicate the positions of electrode ends.

Figure 8 Simulation of 2D rf-only filter, (a) phase, (b) x or y rms position.

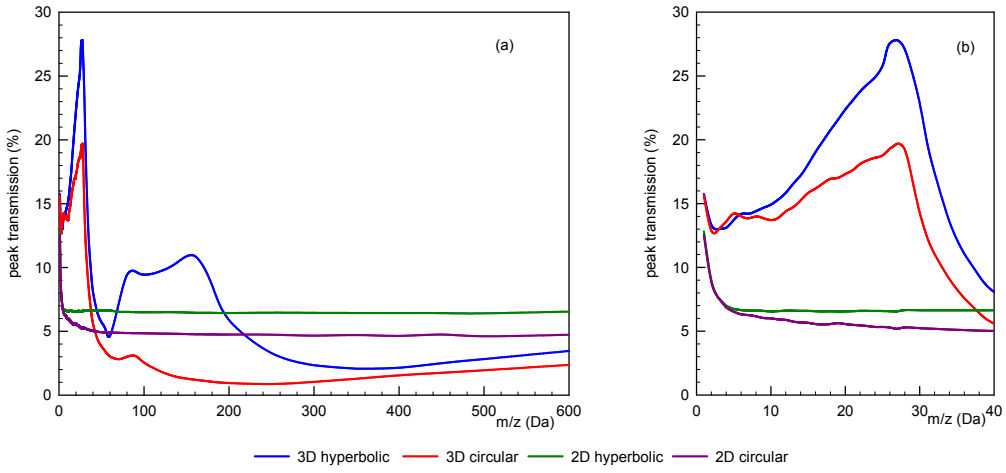


Fig 1

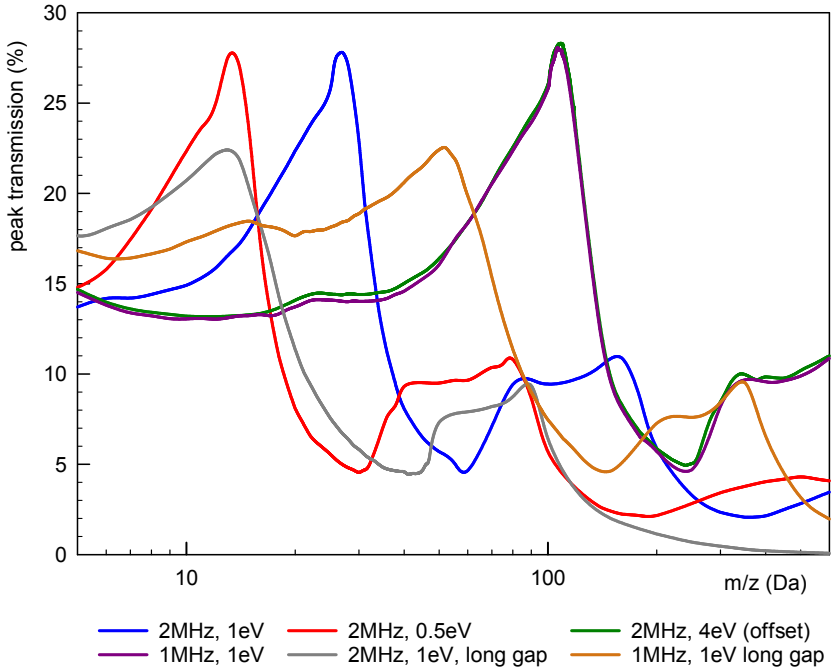


Fig 2

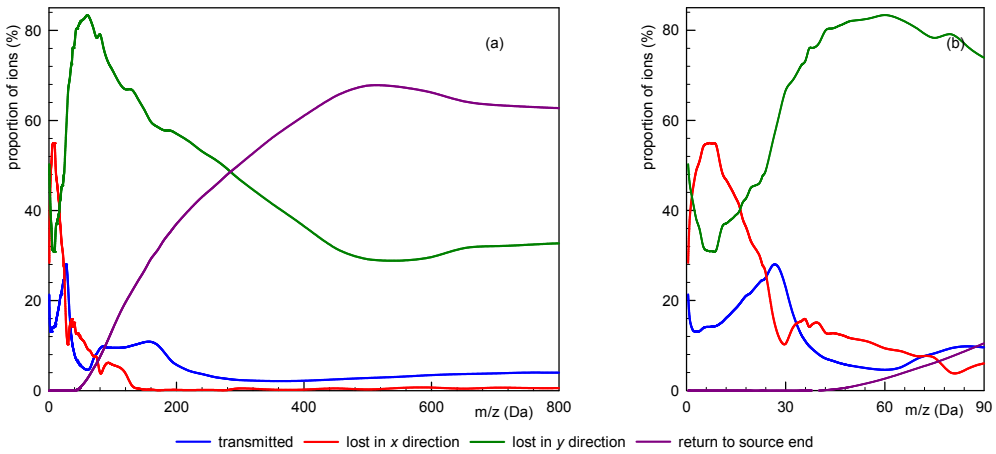


Fig 3

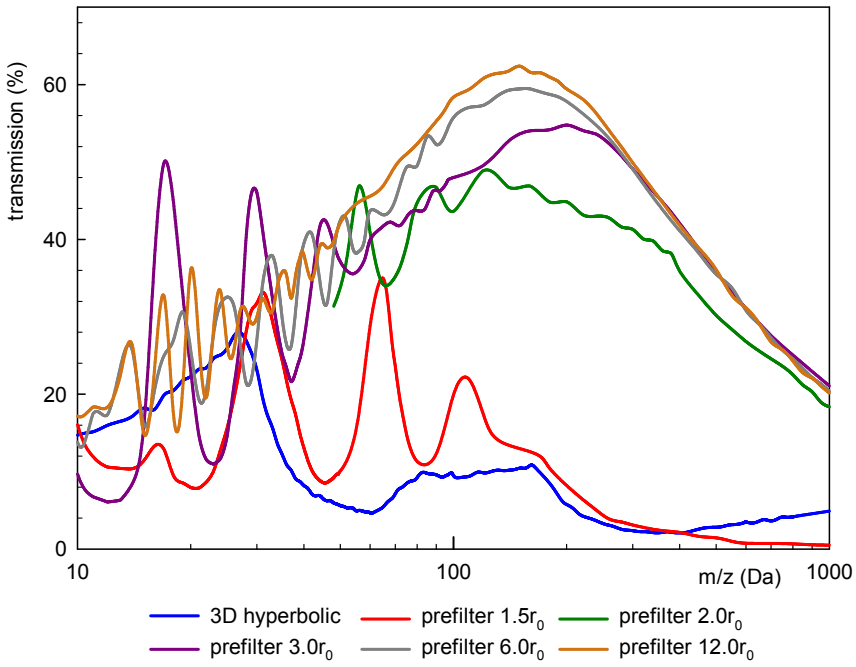
transmission (%)
60
40
20
0
10
100
1000
m/z (Da)
3D hyperbolic
prefilter 1.5r0
prefilter 2.0r0
prefilter 3.0r0
prefilter 6.0r0
prefilter 12.0r0

Fig 4

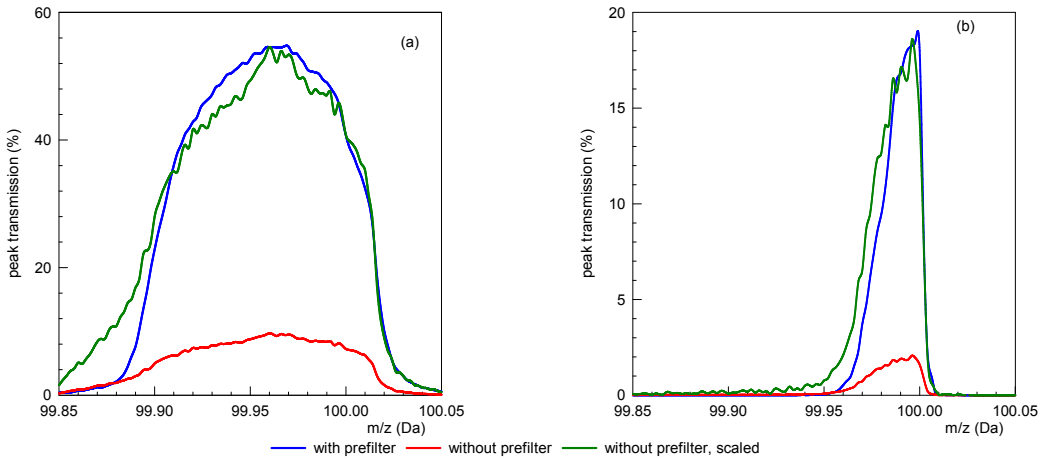
(a)
(b)
peak transmission (%)
60
40
20
0
20
15
10
5
0
99.85
99.90
99.95
100.00
100.05
m/z (Da)
with prefilter
without prefilter
without prefilter, scaled

Fig 5

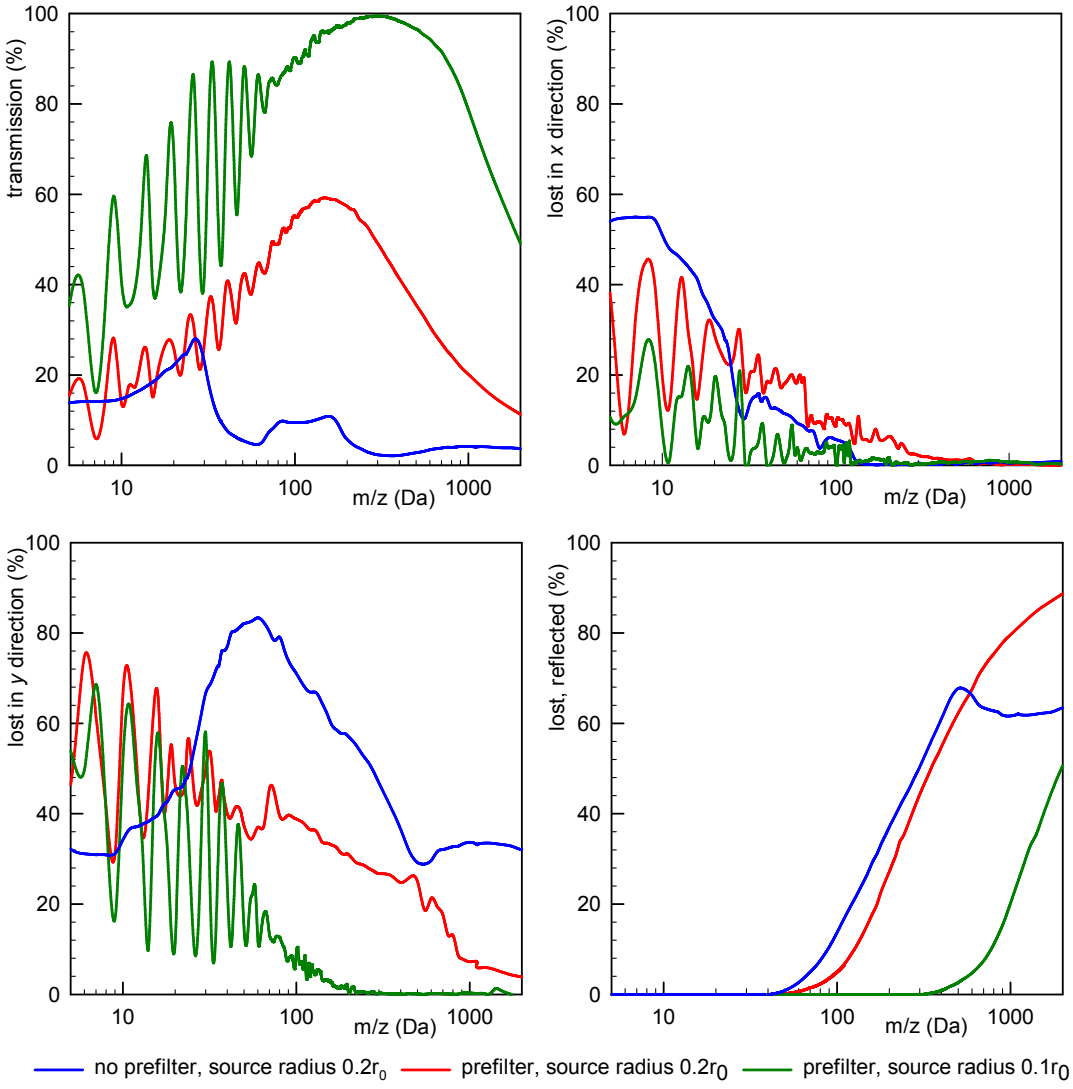
transmission (%)
lost in x direction (%)
lost in y direction (%)
lost, reflected (%)
m/z (Da)
no prefilter, source radius 0.2r0
prefilter, source radius 0.2r0
prefilter, source radius 0.1r0

Fig 6

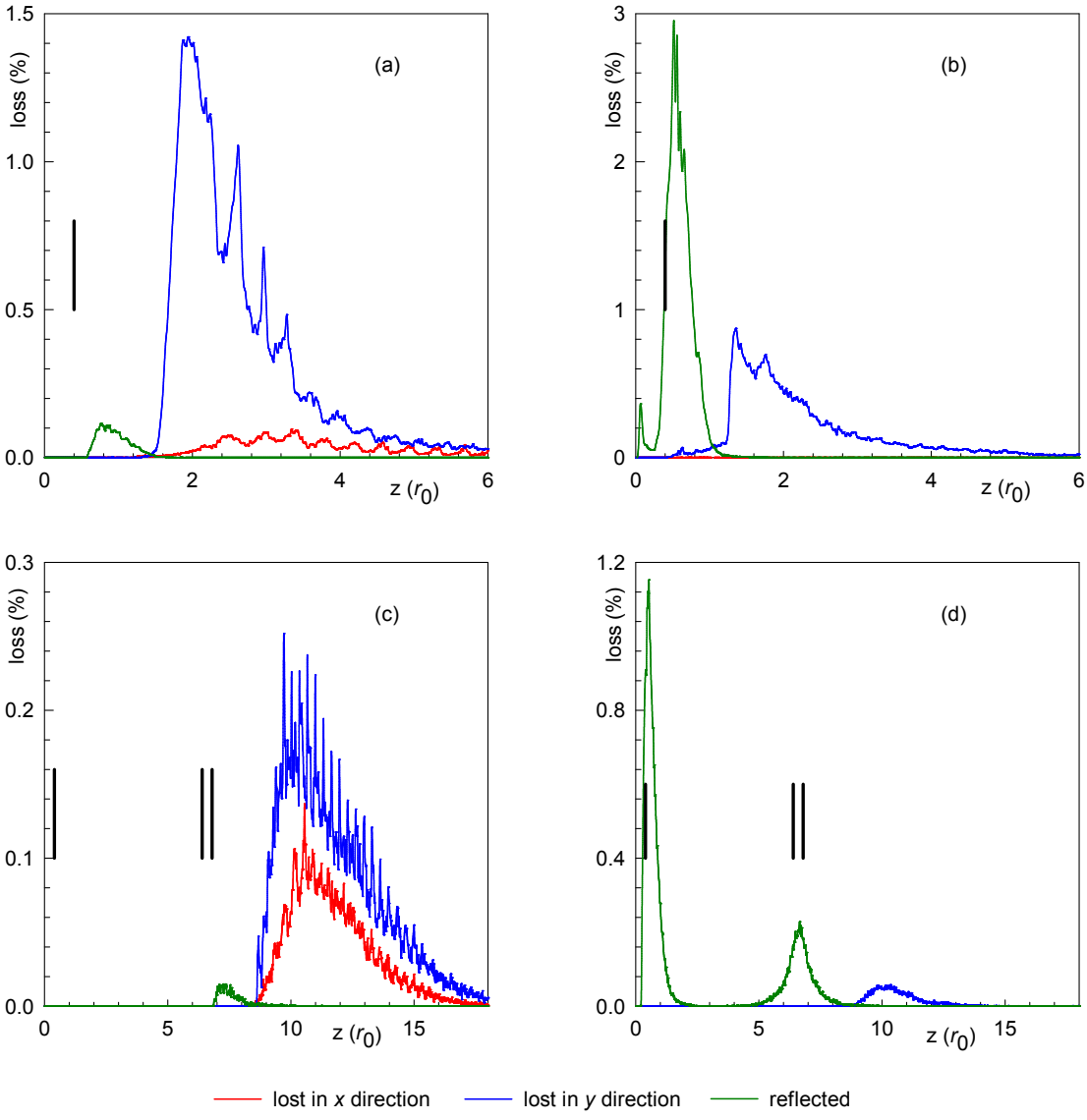
(a)
(b)
(c)
(d)
loss (%)
z ($r_0$)
lost in x direction
lost in y direction
reflected

Fig 7

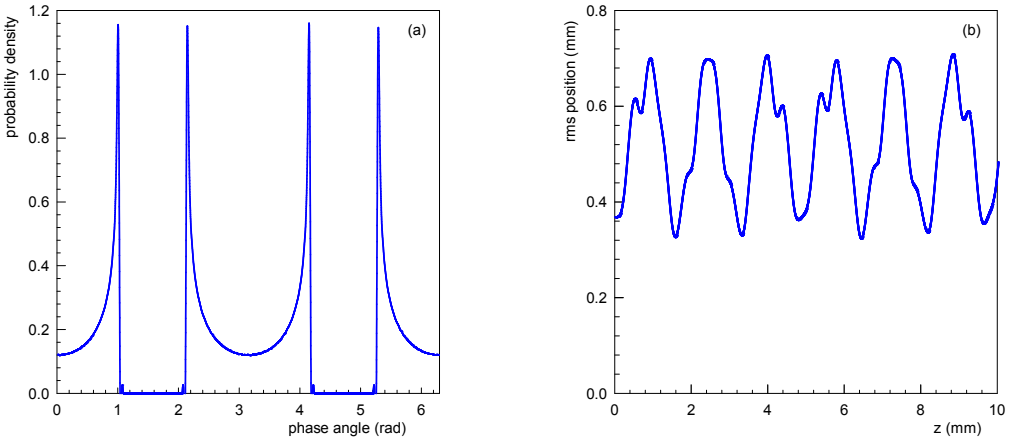
(a)
probability density
phase angle (rad)
(b)
rms position (mm)
z (mm)

Fig 8

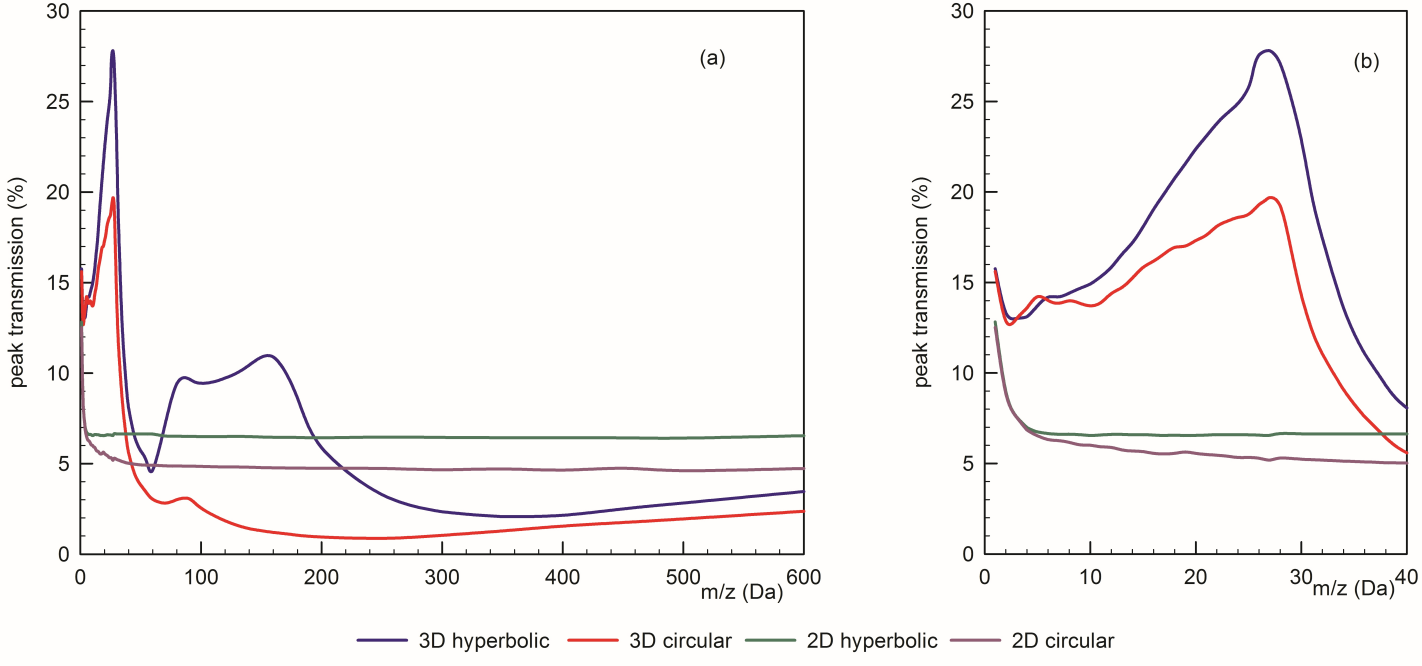
(a)
(b)
peak transmission (%)
m/z (Da)
3D hyperbolic
3D circular
2D hyperbolic
2D circular

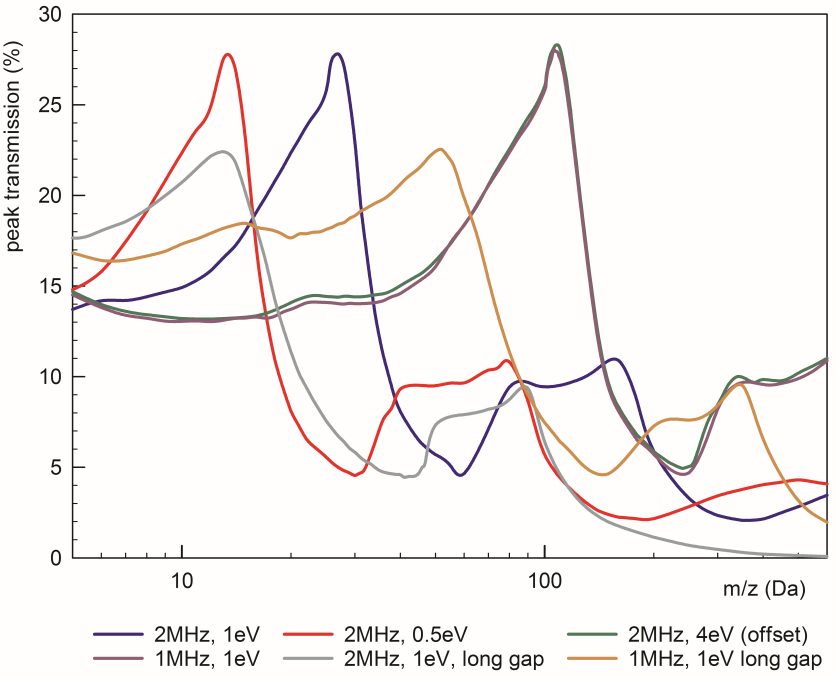
peak transmission (%)
30
25
20
15
10
5
0
10
100
m/z (Da)
2MHz, 1eV
1MHz, 1eV
2MHz, 0.5eV
2MHz, 1eV, long gap
2MHz, 4eV (offset)
1MHz, 1eV long gap

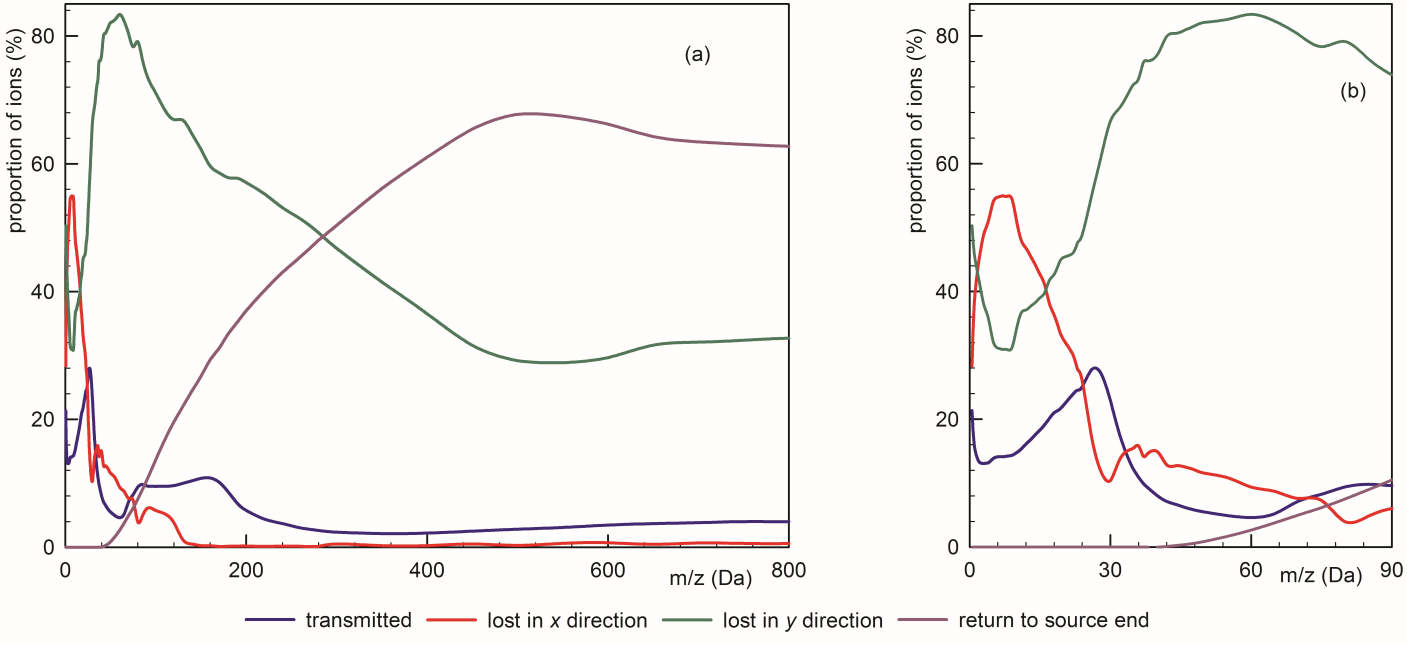
proportion of ions (%)
80
60
40
20
0
(a)
0
200
400
600
800
m/z (Da)
proportion of ions (%)
80
60
40
20
0
(b)
0
30
60
90
m/z (Da)
transmitted
lost in x direction
lost in y direction
return to source end

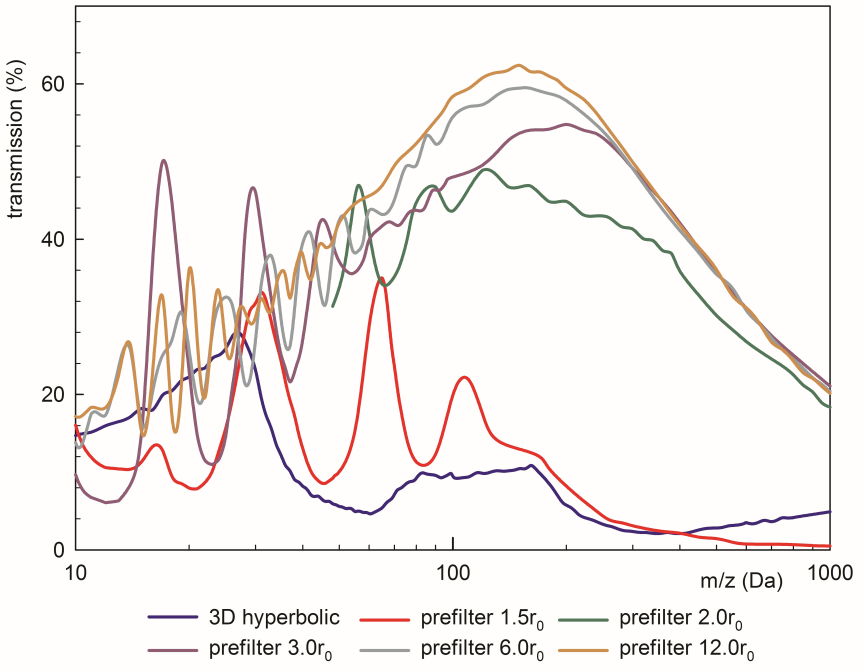
transmission (%)
60
40
20
0
10
100
1000
m/z (Da)
3D hyperbolic
prefilter 1.5r0
prefilter 2.0r0
prefilter 3.0r0
prefilter 6.0r0
prefilter 12.0r0

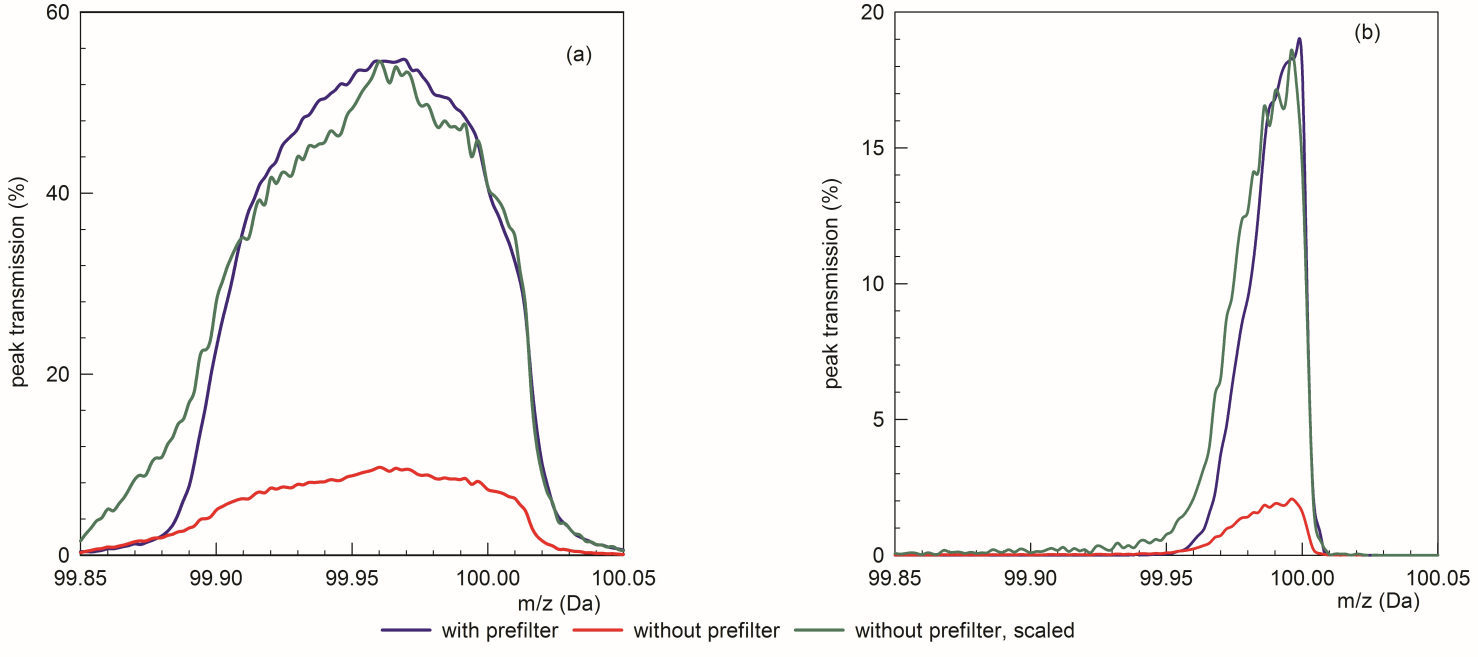
(a)
(b)
peak transmission (%)
m/z (Da)
60
40
20
0
20
15
10
5
0
99.85
99.90
99.95
100.00
100.05
with prefilter
without prefilter
without prefilter, scaled

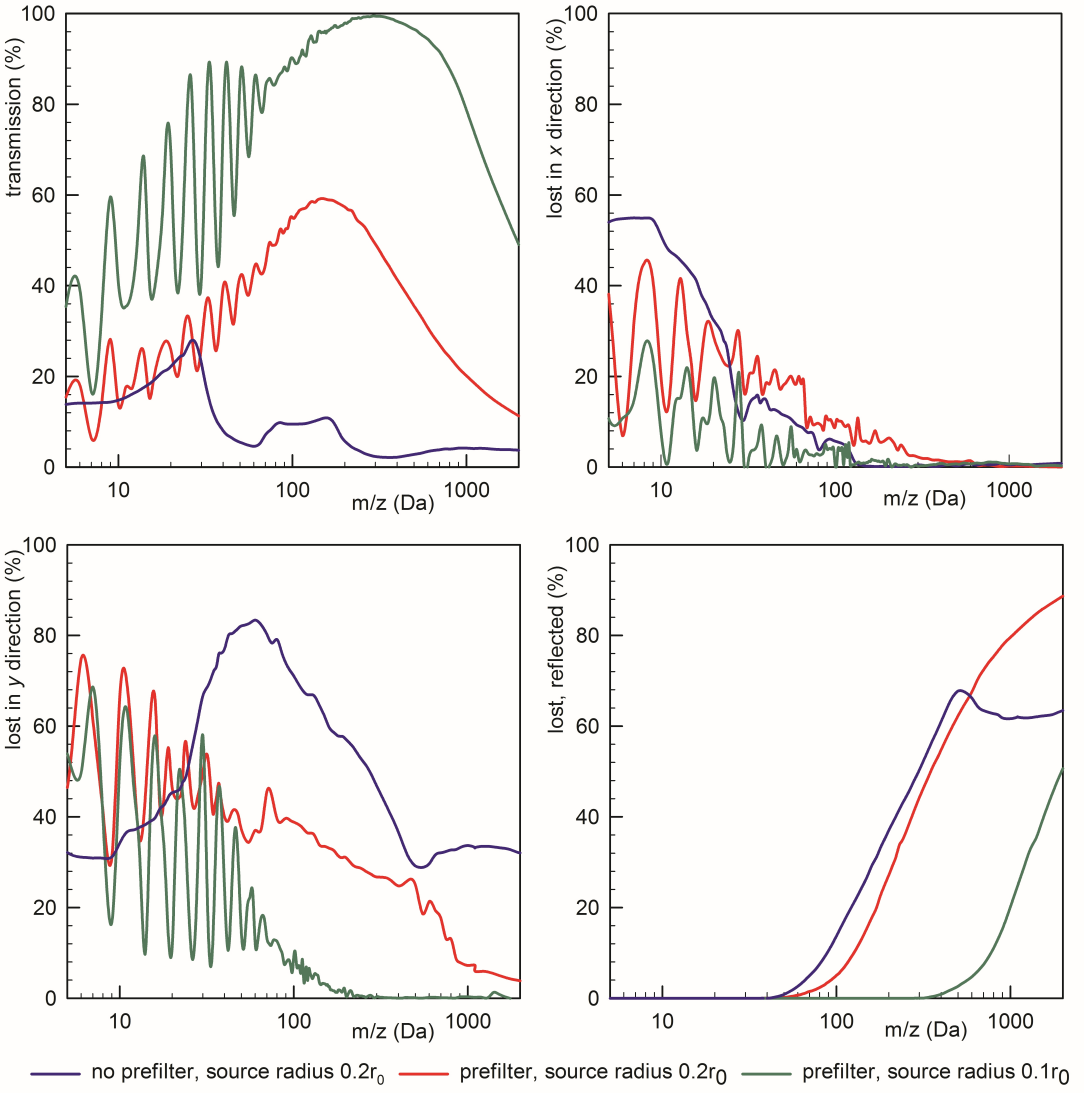
transmission (%)
lost in x direction (%)
lost in y direction (%)
lost, reflected (%)
m/z (Da)
10
100
1000
0
20
40
60
80
100
no prefilter, source radius 0.2r0
prefilter, source radius 0.2r0
prefilter, source radius 0.1r0

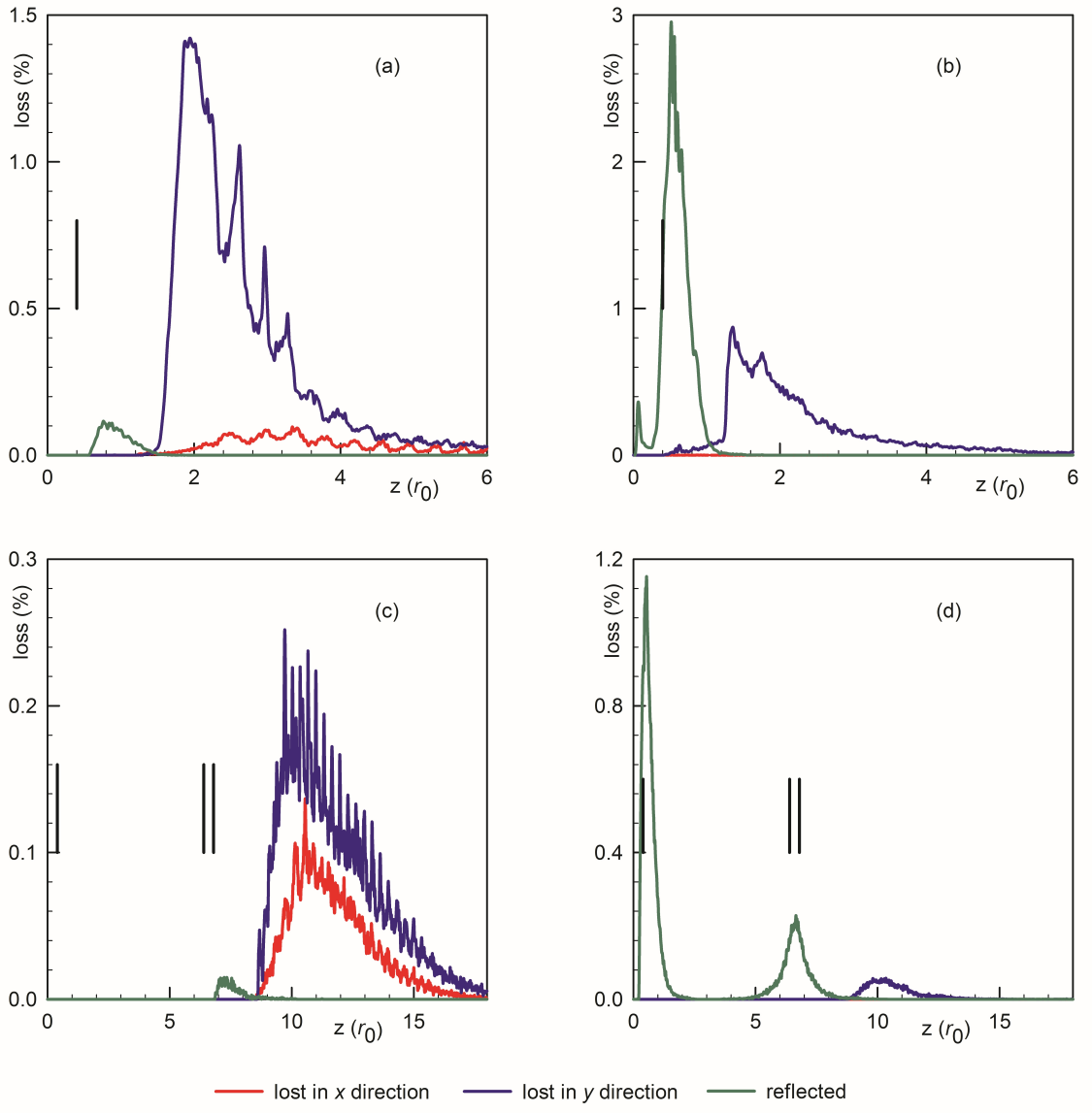
(a)
(b)
(c)
(d)
loss (%)
z ($r_0$)
lost in x direction
lost in y direction
reflected

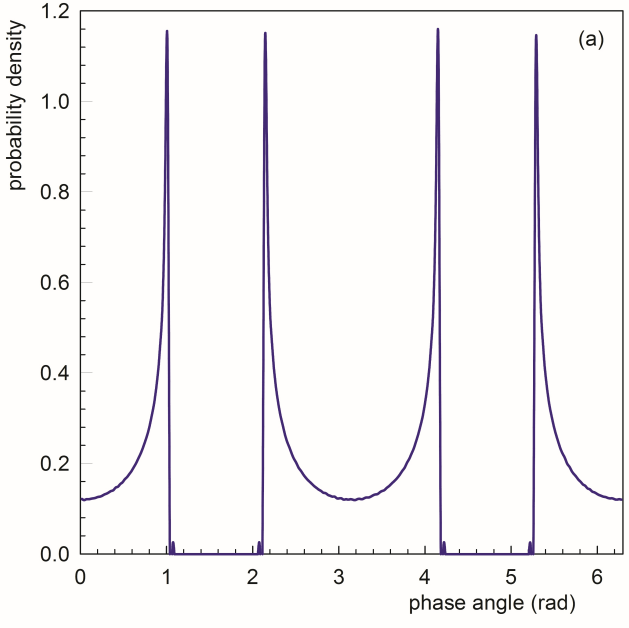
(a)
probability density
1.2
1.0
0.8
0.6
0.4
0.2
0.0
0
1
2
3
4
5
6
phase angle (rad)

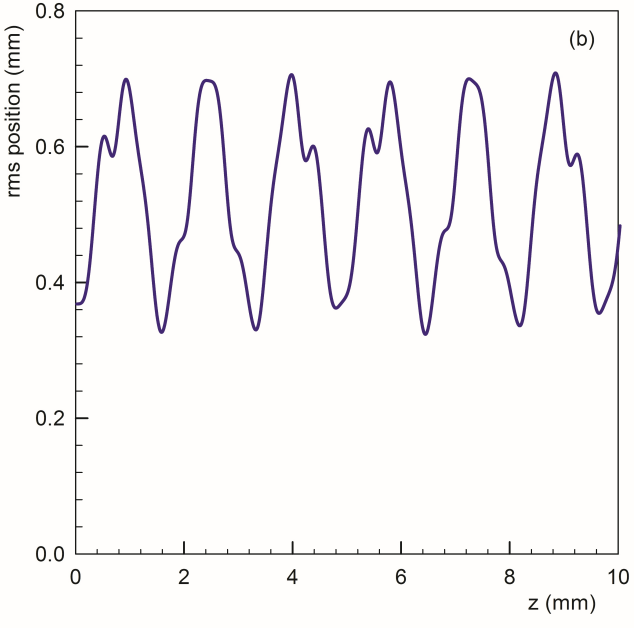
(b)
rms position (mm)
0.8
0.6
0.4
0.2
0.0
0
2
4
6
8
10
z (mm)

- Computer simulation allows a wider range of design parameters to be investigated.
- Accurate 3D fields are used to predict QMF performance with and without prefilters.
- Results confirm that a prefilter increases transmission for low velocity ions.
- The manner and position of ion loss in the fringe field is shown.
- It is shown that the change in axial velocity in the fringe field cannot be ignored.